solutions were treated with Chelex-100 (Bio-Rad) to remove trace metals.
17. Titration with 5,5′-dithiobis(nitrobenzoic acid) (*13*) showed that OP^{26}CAP contained <0.1 mol of accessible cysteine per mole of subunit, indicating that derivatization was at least 90% complete.
18. Nitrocellulose filter binding assays (*5*) indicated that OP^{26}CAP retained high specific DNA binding affinity (a dissociation constant, K_d, of 4.2 ± 0.7 nM). Electrophoretic mobility-shift DNA bending experiments (*19*) indicated that OP^{26}CAP retained nearly full DNA bending activity (DNA bend angle = 116 ± 2°).
19. Y. Zhou, X. Zhang, R. Ebright, *Proc. Natl. Acad. Sci. U.S.A.* **90**, 6081 (1993).
20. Bacteriophage M13mp2-*lacP1*(*lCAP*) was described in (*21*), and λ*i434plac5-P1*(*lCAP*) was constructed according to the procedure of (*22*). DNA-cleaving reactions (110 μl) contained 1 nM DNA substrate, 200 nM OP^{26}CAP (added in five equal amounts at 0, 45, 90, 135, and 180 min), 2.0 μM Cu(II)SO_4, 2.5 mM mercaptopropionic acid, 0.2 mM cAMP, 10 mM MOPS-NaOH (pH 7.3), 200 mM NaCl, bovine serum albumin (50 μg/ml), and 2.2% ethanol. Reactions were initiated by addition of mercaptopropionic acid and proceeded for 6 hours at 37°C. Reactions were terminated by the addition of 2,9-dimethyl-*o*-phenanthroline to 3.0 mM, then phenol-extracted, chloroform-extracted, and ethanol-precipitated. Products in experiments with the 7.2-kb DNA substrate were analyzed by electrophoresis through 0.8% agarose, 1 μM ethidium bromide slab gels; products in experiments with the 48-kb DNA substrate were analyzed by pulsed-field electrophoresis (CHEF; 1.5 V/cm^2; switch time = 2 s; 30 hours at 16°C) through 1% chromosomal-grade agarose slab gels (Stratagene), followed by ethidium bromide staining.
21. X. Zhang, Y. Zhou, R. Ebright, *J. Biol. Chem.* **267**, 8136 (1992).
22. R. Ebright, A. Gunasekera, X. Zhang, T. Kunkel, J. Krakow, *Nucleic Acids Res.* **18**, 1457 (1990); X. Zhang and R. Ebright, *Proc. Natl. Acad. Sci. U.S.A.* **87**, 4717 (1990).
23. M. Koob, E. Grimes, W. Szybalski, *Science* **241**, 1084 (1988); M. Koob and W. Szybalski, *ibid.* **250**, 271 (1990); S. Strobel and P. Dervan, *Nature* **350**, 172 (1991); S. A. Strobel, L. A. Douchette-Stamm, L. Riba, D. E. Housman, P. B. Dervan, *Science* **254**, 1639 (1991); L. Ferrin and R. D. Camerini-Otero, *ibid.*, p. 1494; M. Koob, A. Burkiewicz, J. Kur, W. Szybalski, *Nucleic Acids Res.* **20**, 5831 (1992); T. Povsic, S. Strobel, P. Dervan, *J. Am. Chem. Soc.* **114**, 5934 (1992).
24. R. Ebright *et al.*, *Proc. Natl. Acad. Sci. U.S.A.* **84**, 6083 (1987).
25. Strain XAE4000 was constructed by integration of λ*i434plac5-P1*(*lCAP*) at the λ*att* site [procedure in (*22*)]. There are no consensus DNA sites for CAP in wild-type *E. coli* (*3*). DNA sites for CAP in wild-type *E. coli* have a minimum of five differences from the consensus DNA site and exhibit one to three orders of magnitude lower affinities (*5*).
26. Agarose plugs containing genomic DNA of strain XAE4000 were prepared with InCert agarose (FMC BioProducts) and the procedure of the manufacturer with two modifications: (i) proteinase-K digestion was for 72 hours, and (ii) residual low molecular weight contaminants were removed by pulsed-field electrophoresis (TAFE in a matrix of 1% chromosomal-grade agarose; 1.5 V/cm^2; switch time = 15 s; 12 hours at 4°C) followed by equilibration in 500 μl of 10 mM tris-HCl (pH 7.9), 150 mM NaCl, 10 mM $MgCl_2$, and 0.01% Triton X-100. Digestions with Not I (500 μl; 14 hours at 37°C) contained an agarose plug with DNA substrate, 30 U Not I (New England Biolabs), 50 mM tris-HCl (pH 7.9), 100 mM NaCl, 10 mM $MgCl_2$, and 1 mM dithiothreitol. Digestions with copper:OP^{26}CAP (200 μl; 3 hours at 37°C) contained an agarose plug with DNA substrate, 120 nM OP^{26}CAP (added in two equal amounts at 0 and 1.5 hours), 0.2 mM cAMP, 1 μM Cu(II)SO_4, 2.5 mM mercaptopropionic acid, 10 mM MOPS-NaOH (pH 7.3), and 200 mM NaCl. The copper:OP^{26}CAP digestions were initiated by addition of mercaptopropionic acid and were terminated by transfer of agarose plugs to 500 μl of reaction buffer plus 3 mM 2,9-dimethyl-*o*-phenanthroline at 4°C. Reaction products were analyzed by pulsed-field electrophoresis (TAFE; 1.5 V/cm^2; switch time = 15 s; 12 hours at 4°C) through 1% chromosomal-grade agarose slab gels, followed by transfer to Nytran (Schleicher & Schuell) and Southern hybridization with ^{32}P-labeled probes corresponding to the left and right arms of integrated λ*i434plac5-P1*(*lCAP*) prophage [prepared by nick-translation of Xba I–digested λ*i434plac5-P1*(*lCAP*)].
27. Reactions were performed essentially as in (*20*). The DNA substrate was 40-bp synthetic DNA fragment lCAP 5′ end-labeled with ^{32}P (*5*). The OP^{26}CAP concentration was 80 nM (added in a single amount). Products were analyzed by denaturing gel electrophoresis through 20% polyacrylamide, 8.3 M urea slab gels, followed by autoradiography.
28. C. Kang and M. Inouye, *Biotechniques* **15**, 659 (1993).
29. Y. Kim, J. C. Grable, R. Love, P. J. Greene, J. M. Rosenberg, *Science* **249**, 1307 (1990); D. R. Lesser, M. R. Kurpiewski, L. Jen-Jacobson, *ibid.* **250**, 776 (1990); F. Winkler, *Curr. Opin. Struct. Biol.* **2**, 93 (1992); F. Winkler *et al.*, *EMBO J.* **12**, 1781 (1993); I. B. Vipond and S. Halford, *Mol. Microbiol.* **9**, 225 (1993).
30. I. Weber and T. Steitz, *Nucleic Acids Res.* **12**, 8475 (1984).
31. ———, *J. Mol. Biol.* **198**, 311 (1987). Accession code is 3GAP.
32. L. Battaglia, A. Bonamartini Corradi, G. Marcotrigiano, G. Pellacani, *Acta Cryst.* **B33**, 3886 (1977). Accession code is ACGLCU.
33. DNA FIT MAN; J. Warwicker, Yale University.
34. We thank D. Axelrod and J. Messing for access to a pulsed-field gel electrophoresis apparatus. This work was supported by NIH grant GM41376, a Searle Scholar Award, and a Boehringer Mannheim GmbH research contract to R.H.E.

1 March 1994; accepted 10 June 1994

Oscillations of Membrane Current and Excitability Driven by Metabolic Oscillations in Heart Cells

Brian O'Rourke, Brian M. Ramza, Eduardo Marban*

Periodic changes in membrane ionic current linked to intrinsic oscillations of energy metabolism were identified in guinea pig cardiomyocytes. Metabolic stress initiated cyclical activation of adenosine triphosphate–sensitive potassium current and concomitant suppression of depolarization-evoked intracellular calcium transients. The oscillations in membrane current and excitation-contraction coupling were linked to oscillations in the oxidation state of pyridine nucleotides but were not driven by pacemaker currents or alterations in the concentration of cytosolic calcium. Interventions that altered the rate of glucose metabolism modulated the oscillations, suggesting that the rhythms originated at the level of glycolysis. The energy-driven oscillations in potassium currents produced cyclical changes in the cardiac action potential and thus may contribute to the genesis of arrhythmias during metabolic compromise.

Periodic rhythms underlie biological processes as diverse and fundamental as neuronal firing, secretion, and muscle contraction. Cellular oscillators have been broadly categorized by the location of the primary rhythm generator, either at the surface membrane or at an intracellular site (*1*). Extracellular and intracellular inputs modulate the activity of both types of oscillator, and interactions between the two may be necessary for a maintained response (*2*). Descriptions of several oscillatory biochemical pathways have lent support to the notion that single rate-controlling enzymes possess regulatory properties capable of supporting stable nonequilibrium oscillatory states under defined conditions (*3*). One such system is the glycolytic oscillator, which is primarily controlled by phosphofructokinase (*4*). The ubiquitous distribution of glycolytic enzymes has motivated proposals that the oscillator could mediate various oscillatory physiological behaviors, including slow waves of contraction in smooth muscle (*5*), bursting electrical activity in *Aplysia* neurons (*6*), and insulin release from the β islet cells of the pancreas (*7*).

Our results describe a metabolic oscillator revealed by substrate deprivation that drives oscillations in the adenosine triphosphate (ATP)–sensitive potassium current and in the amplitude of depolarization-evoked increases in intracellular Ca^{2+} concentration (Ca^{2+} transients) in ventricular myocytes. Examination of the mechanism of this phenomenon indicates that the glycolytic oscillator may be the primary rhythm generator underlying the observed changes in membrane currents and excitation-contraction coupling.

Membrane current and fluorescence were measured in guinea pig ventricular myocytes equilibrated with intracellular

The Johns Hopkins University, Department of Medicine, Division of Cardiology, 844 Ross Building, 720 North Rutland Avenue, Baltimore, MD 21205, USA.

*To whom correspondence should be addressed.

and extracellular solutions containing physiological concentrations of ions (*8*). When external glucose is supplied, such myocytes respond to depolarizations with little alteration of Na^+, Ca^{2+}, and K^+ currents for 30 min or more (*9*). When fuel substrates were omitted from the bathing medium, large periodic increases in a background membrane conductance were initiated. In each cycle of oscillation, the current developed over 30 s, peaked briefly, and resolved within the next 60 s (Fig. 1A). In the absence of external substrate, spontaneous oscillations in membrane conductance were observed in 42 of 96 myocytes (44%), with a slightly higher percentage obtained in a subgroup of myocytes equilibrated with internal solutions having less than 5 mM ATP. In myocytes that did not oscillate spontaneously at the onset of the experiment, oscillatory membrane currents were often initiated after prolonged observation or after perturbations of intracellular metabolites. Simultaneous measurement of intracellular Ca^{2+} concentration revealed that peak systolic Ca^{2+} (that is, during membrane depolarization) was suppressed in phase with the development of the oscillatory current without a change in diastolic Ca^{2+} (Fig. 1, A and B). This reduction in the amplitude of the Ca^{2+} transient was reversed when the background current returned to baseline. The peak-to-peak period of spontaneous oscillations for eight different cells averaged 1.66 ± 0.21 min (mean ± SD), with the predominant pattern observed being pseudosinusoidal (*10*). Self-sustaining oscillations in current and in the amplitude of the Ca^{2+} transient could be observed for more than 2 hours.

Analysis of the current-voltage relation for background currents during membrane voltage ramps (Fig. 2A) revealed that the reversal potential of the background current at the peak of an oscillation was the same as that during the nadir. The reversal potential of the background currents always remained near the estimated equilibrium potential for potassium (E_K = −86 mV for the experimental solutions) and could not be explained by alterations in the membrane conductance of other cations or that of chloride. Because the oscillating K^+ current showed weak inward rectification at positive potentials and was observed only during metabolic stress, ATP-sensitive potassium channels ($I_{K,ATP}$) were suspected as mediators of the response. We tested this possibility by applying the ATP-sensitive potassium channel blocker glibenclamide to a myocyte undergoing spontaneous oscillations. Consistent with a mechanism involving $I_{K,ATP}$, glibenclamide abruptly halted the oscillations (Fig. 2B) (*11*). Changes in membrane potential or in resting intracellular Ca^{2+} concentration were not required to support the oscillations in $I_{K,ATP}$. In a myocyte undergoing spontaneous oscillations of membrane current and Ca^{2+} transient amplitude during depolarizing steps (Fig. 2C), the membrane potential was held constant at −80 mV for 10 min. Elimination of voltage-activated currents abolished the intracellular Ca^{2+} transient without affecting the oscillations in holding current (Fig. 2C). Thus, the oscillatory phenomenon neither requires voltage changes nor does it rely on feedback control by intracellular Ca^{2+} (*1, 2, 12, 13*).

Stable oscillations in the flux of substrates through glycolysis have been observed (*4, 14, 15*). In intact yeast, glycolytic oscillations can be recorded by monitoring the concentration of reduced nicotinamide adenine dinucleotides (NADs) [primarily the reduced form of NAD^+ (NADH)] with fluorescence spectroscopy (*16*). We found that the oscillations in $I_{K,ATP}$ were correlated with transient decreases in NADH (Fig. 3A). Analysis of the first derivative of the time course of oscillations in current and NADH indicated that the decrease in NADH consistently preceded the increase in membrane currents (Fig. 3B), suggesting that a change in the rate of energy metabolism initiated the change in membrane conductance.

Further support for this idea was obtained by altering the rates of glycolysis or oxidative phosphorylation with exogenous substrates or metabolic inhibitors. Provision of glucose to cardiomyocytes displaying the oscillatory response interrupted the cycle of oscillations in the majority of cases (Fig. 4A): in some cells, only a strong amplitude damping effect was observed on exposure to glucose, with little effect on the frequency (Fig. 4B). Although the oscillatory response is closely associated with glycolytic flux, oscillations of mitochondrial function [reported in isolated mitochondria (*17*)] could not be excluded as a potential source of oscillation. However, two pieces of evidence argue against mitochondria as the primary site of the oscillator.

First, a high concentration of glutamate was the main anion in the intracellular solution in most experiments, thus providing a substrate for oxidative metabolism by means of conversion to α-ketoglutarate by glutamate dehydrogenase (*18*). Substitution of the glutamate with chloride did not prevent the occurrence of spontaneous current oscillation, indicating that the key factor was not oxidative substrate availability.

Second, we also inhibited glycolysis and oxidative phosphorylation in a cell exhibiting spontaneous oscillations (Fig. 5A). In-

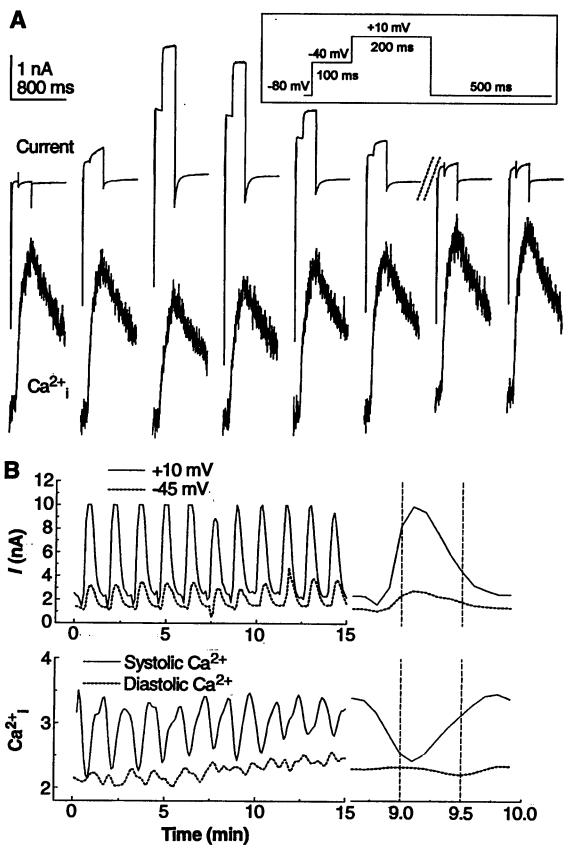

Fig. 1. Changes in membrane current and intracellular Ca^{2+} (Ca^{2+}_i) transients during metabolic oscillations. (**A**) Upper panel shows membrane currents recorded when the voltage protocol (inset) was repeated every 6 s during a single oscillatory cycle in a myocyte bathed in substrate-free medium. Rapidly inactivating inward Na^+ currents are the abrupt downward spikes at the onset of the depolarization to −40 mV. L-type Ca^{2+} currents are apparent in the second depolarization to +10 mV but are obscured by the large outward current at the peak of the oscillation. The noisier traces in the lower panels are Ca^{2+} transients evoked y the membrane depolarizations. Dashed lines indicate that six records of the sequence in both panels have been omitted. (**B**) (Upper panel) The time course of changes in membrane current (*I*), and (lower panel) systolic Ca^{2+} (the peak fluorescence during a depolarizing pulse) and diastolic Ca^{2+} (fluorescence at the holding potential) during 11 oscillations. The upper panel is a sequential plot of currents at the holding potential (−45 mV) and at +10 mV. Current values were taken just before and at the end of a depolarizing pulse to +10 mV (repeated every 6 s). The lower panel displays the corresponding values of diastolic Ca^{2+} and systolic Ca^{2+}. An expanded plot of a single oscillation is shown to the right of each data set (Ca^{2+} values are uncalibrated fluorescence units).

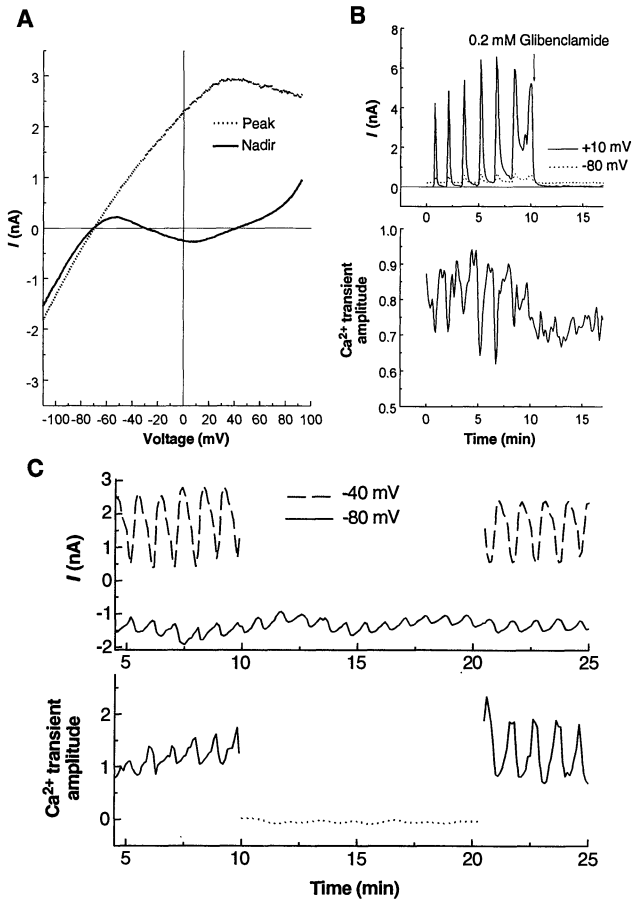

Fig. 2. Identification of the background current as $I_{K,ATP}$. (**A**) Voltage ramps from +100 mV to −110 mV were repeated every 4 s during membrane current oscillations. Selected records show the current-voltage relation between the oscillations (solid line) and at the peak of the oscillating background current (dotted line). The reversal potential was −70 mV and remained unchanged during the oscillations. (**B**) Interruption of the oscillations in current (upper panel) by the ATP-sensitive K^+ channel blocker glibenclamide. The Ca^{2+} transient amplitude (lower panel) is the difference between the systolic and diastolic fluorescence values. (**C**) Spontaneous oscillations in membrane current in response to a voltage protocol like that in Fig. 1A (upper panel) and in the absence of depolarizing pulses (denoted by the interruption in −40-mV plot). Ca^{2+} transients ceased when the depolarizations were suspended (lower panel). The solid line is the difference between the fluorescence maximum during depolarization and the fluorescence just before depolarization (Ca^{2+} transient amplitude), whereas the dotted line is the fluorescence difference calculated from similar time points in the absence of depolarizing pulses (−80-mV holding potential).

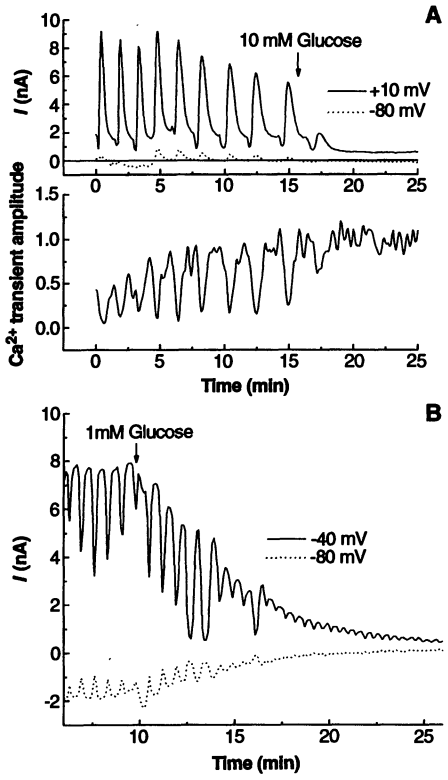

Fig. 4. Effect of extracellular glucose on oscillations in $I_{K,ATP}$ and Ca^{2+} transient amplitude; (**A**) 10 mM glucose; (**B**) effect of 1 mM glucose on membrane current.

hibition of glycolysis with the glucose analog 2-deoxyglucose interrupted oscillations, although there was still sufficient ATP [either from the pipette solution or the oxidative metabolism of glutamate (*19*)] to prevent activation of ATP-sensitive K^+ channels. The same myocyte was then exposed to the mitochondrial uncoupler 2,4-dinitrophenol. This resulted in an increase in diastolic Ca^{2+} and suppression of the Ca^{2+} transient that was followed shortly thereafter by the development of a large, sustained outward current, reflecting the activation of $I_{K,ATP}$ in response to severe ATP depletion (Fig. 5A). Restoration of both glycolytic and oxidative metabolism by washing out dinitrophenol in the presence of glucose rapidly reversed the effects of dinitrophenol. A series of eight damped oscillations were then observed after a short delay. The occurrence of oscillations in $I_{K,ATP}$ and excitation-contraction coupling during recovery from severe metabolic inhibition indicates the potential importance of this phenomenon during the reperfusion of ischemic cardiac tissues, when the risk of arrhythmias is high (*20*).

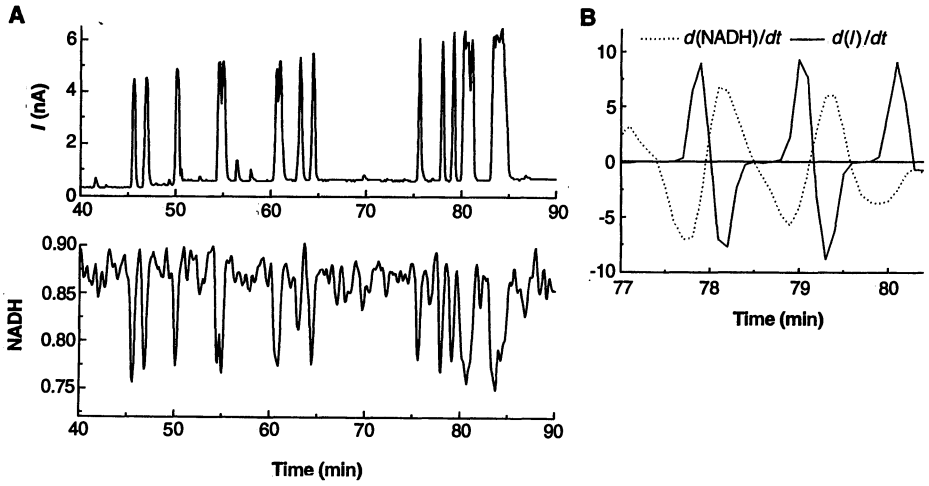

Fig. 3. Correlation between $I_{K,ATP}$ oscillations and NADH fluorescence. (**A**) NADH fluorescence oscillations (lower panel; uncalibrated fluorescence units) corresponding to oscillations in membrane current (upper panel; current at −40 mV). (**B**) Phase shift between the first derivative plots of NADH (dashed line; scaled to match the derivative of current) and membrane current (solid line).

Our results indicate that, over a crucial range of glycolytic rates, an oscillatory pattern can be sustained—a decrease in flux below or an increase above that range pushes the system out of the oscillatory domain. This interpretation agrees with models of the glycolytic oscillator (*21*), in particular, the critical dependence of glycolytic oscillations on substrate influx rate (*22*). Although resistant to deviation from the mean autonomous oscillatory frequency over a range of periodic substrate influx rates, entrainment of the glycolytic oscillator to the input frequency as well as chaotic behavior occurs at specific input frequencies

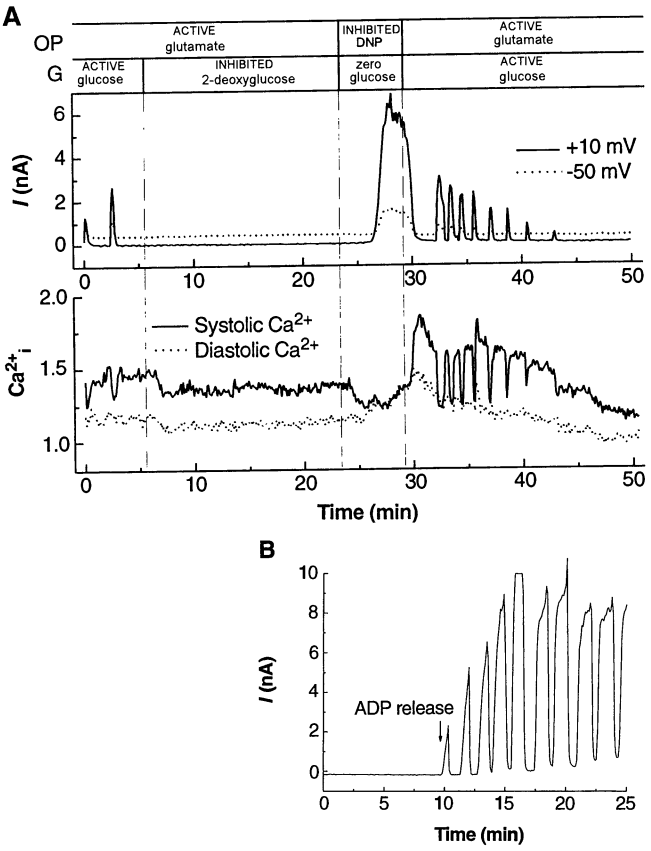

Fig. 5. Influence of metabolic modulators on oscillations of $I_{K,ATP}$ and Ca^{2+} transients. (**A**) Effects of glycolytic inhibition (10 mM 2-deoxyglucose), uncoupling mitochondrial energy production [0.2 mM dinitrophenol (DNP)], and recovery from inhibition on oscillations in current (upper panel) and systolic Ca^{2+}_i (lower panel). The combined effects of external and internal substrates and inhibitors on oxidative phosphorylation (OP) and glycolysis (G) are indicated above. (**B**) Flash photolysis of caged ADP in a cell that was not previously oscillating. Internal solution contained 0.2 mM ATP and 1 mM caged ADP.

(*23*). In cardiac cells, which normally rely on oxidative metabolism, another type of entrainment must be considered. The cyclical changes in adenine nucleotides, NADH, and pyruvate generated in bursts by glycolysis may serve to entrain mitochondrial function to the cytoplasmic oscillator, thus amplifying the effect. Feedback on the glycolytic oscillator by oxidative metabolism (*24*) may also modulate the oscillatory response.

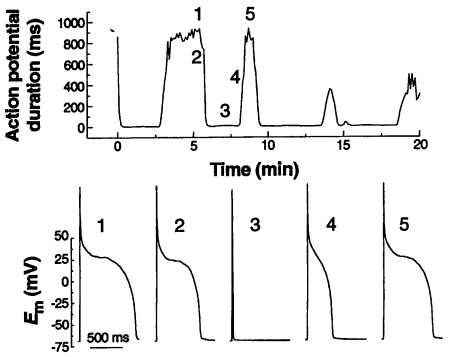

Fig. 6. Effects of metabolic oscillations on electrical excitability. Upper panel, the action potential duration (90% repolarization time) for a series of action potentials evoked by brief current injections (at 6-s intervals) in a current-clamped cardiomyocyte. Lower panel, selected action potentials recorded at the time points indicated by the numbers on the upper panel. The brief depolarization in 3 is the stimulus artifact. E_m is the cell membrane potential.

Oscillations in the concentrations of glycolytic intermediates have been measured in cell-free extracts of skeletal muscle (*25*), heart (*15*), yeast (*26*), and blowfly thorax (*14*). In all of these systems, phosphofructokinase (PFK) has been identified as the major control point for maintaining stable nonequilibrium oscillations in glycolysis. The activity of PFK is regulated by the positive allosteric effectors adenosine monophosphate (AMP), adenosine diphosphate (ADP), inorganic phosphate (P_i), and the negative effectors ATP and citrate. Allosteric modulators of PFK have been shown to alter the frequency and amplitude of the oscillations, often in a phase-dependent manner (*27*). We tested whether the observed oscillations in membrane current responded to interventions that alter the activity of the glycolytic oscillator. If changes in the ATP/ADP ratio trigger oscillations, we reasoned that a rapid increase in cytosolic ADP might initiate the response. This prediction was borne out by experiments in which the concentration of cytosolic ADP was rapidly increased by flash photolysis of intracellular caged ADP. In a cell that was not oscillating, ADP release immediately induced a series of oscillations of steadily increasing amplitude (Fig. 5B) (*28*).

The large oscillations of membrane current measured under voltage clamp conditions implied that electrical excitability would be altered cyclically. This prediction was tested by recording action potentials in a cell that showed spontaneous oscillations in $I_{K,ATP}$ (Fig. 6). Whereas the resting membrane potential (close to E_K) was minimally influenced by the oscillatory increases in background potassium conductance, cyclical changes in the repolarization phase of the action potential were observed, and periods of inexcitability paralleled the time course of current oscillations.

Our results indicate that oscillations of energy metabolism are capable of modulating cardiac excitability and intracellular Ca^{2+} homeostasis. In mammalian cells, the strongest evidence of a physiological consequence of primary metabolic oscillations has been in the process of excitation-secretion coupling in pancreatic cells, where the glycolytic oscillator has been proposed to influence the bursting pattern of membrane depolarizations mediating insulin release (*7*). We have found that metabolic oscillations often occur in myocardial cells subjected to reversible metabolic stress, induced after substrate deprivation or on recovery from metabolic inhibition by chemical agents. Interruption of coronary flow produces comparable metabolic effects in the intact heart during an ischemic episode. Temporal alterations in the shape and duration of the cardiac action potential in individual cells or regions of the myocardium would be expected to greatly increase the susceptibility to fatal ventricular arrhythmias (*20*). The oscillatory phenomenon may therefore represent a cellular mechanism contributing to the contractile and electrical dysfunctions associated with myocardial ischemia.

REFERENCES AND NOTES

1. R. W. Tsien, R. S. Kass, R. Weingart, *J. Exp. Biol.* **81**, 205 (1979).
2. R. W. Tsien and R. Y. Tsien, *Annu. Rev. Cell Biol.* **6**, 715 (1990).
3. V. Andrés, V. Schultz, K. Tornheim, *J. Biol. Chem.* **265**, 21441 (1990).
4. B. Hess and T. Plesser, *Ann. N.Y. Acad. Sci.* **316**, 203 (1979); K. Tornheim, *J. Theor. Biol.* **79**, 491 (1979).
5. J. A. Connor, *J. Exp. Biol.* **81**, 153 (1979).
6. R. W. Meech, *ibid.*, p. 93.
7. B. E. Corkey *et al.*, *J. Biol. Chem.* **263**, 4254 (1988).
8. Cell isolation and experimental apparatus were as described [P. H. Backx, B. O'Rourke, E. Marban, *Am. J. Hypertens.* **4**, 416S (1991)]. Ventricular myocytes were enzymatically isolated and stored at room temperature in a high-potassium solution containing 120 mM K-glutamate, 25 mM KCl, 1 mM $MgCl_2$, 10 mM Hepes, 0.1 mM EGTA, and 10 mM glucose. Before each experiment, cells were washed in a modified Tyrode's solution containing 140 mM NaCl, 5 mM KCl, 2 mM $CaCl_2$, 1 mM $MgCl_2$, and 10 mM Hepes (pH 7.4 with NaOH at 22° to 23°C). The isolation technique [M. Mitra and M. Morad, *Am. J. Physiol.* **249**, H1056 (1985)] yields Ca^{2+}-tolerant, quiescent myocytes. Substrate deprivation had no untoward effects on the appearance of the myocytes; cells remained rod-shaped with clearly defined striations. Patch electrodes were 1.5-mm borosilicate glass with tip resistances of 0.5 to 2 megohm. After a gigaohm seal was formed, whole-cell clamp was achieved by breaking the membrane with gentle suction. Series resistance generally ranged from 4 to 10 megohms, 70 to 80% of which

was compensated electronically, thus reducing the maximum error of the voltage clamp to approximately 10 mV for the largest currents recorded (~10 nA). The intracellular solution contained 120 mM K-glutamate, 20 mM KCl, 10 mM Hepes, 0.02 to 0.03 mM Calcium Green (Molecular Probes, Eugene, OR), 10 mM Na^+, 5.5 mM total Mg, and 0.2, 1, or 5 mM ATP (Na^+ and Mg^{2+} concentrations were held constant with Na^+ or Mg^{2+} salts of ATP; pipette pH adjusted to 7.2 with KOH). Calcium Green was replaced with EGTA when NADH fluorescence was measured. In some experiments, 1 mM caged ATP or 1 mM caged ADP were added to the pipette solution and photolyzed with a xenon flash lamp. A continuous xenon arc lamp was used to provide excitation light (485 nm) for Calcium Green; fluorescence emission (530 nm) was detected with a photomultiplier tube. NADH fluorescence was measured at 460 nm in myocytes illuminated with 350 nm ultraviolet light. Membrane ionic currents and fluorescence signals were acquired by a digital interface controlled by a personal computer and customized software. Experiments were done in accordance with institutional guidelines regarding the care and use of animals.

9. B. Belles, C. O. Malécot, J. Hescheler, W. Trautwein, *Pflueg. Arch.* **411**, 353 (1988).
10. In the majority of the experiments, the frequency and amplitude of the spontaneous oscillations remained constant over long periods of time and could be approximated by a sinusoidal function; however, in several instances, an additional frequency damping factor of 10 to 20% over a 10-min time period was needed to adequately describe the data. A few cells displayed oscillations with an irregular phase, amplitude, or both (Fig. 3A). These examples of unusual patterns of oscillation are similar to those observed in cell-free extracts when the substrate influx rate is altered and may be explained by variability in the amounts of endogenous energy stores in the isolated myocytes. Glycogen, which is partially depleted by the isolation process [V. Chen, K. H. McDonough, J. J. Spitzer, *Biochim. Biophys. Acta* **846**, 398 (1985)], presumably supports the cyclical alterations in metabolic rate by providing substrate at a slower rate than in the presence of glucose. Differences in rates of glucose transport or glycogenolysis among cells may account for the variable sensitivities to external glucose. The reduction in amplitude of the Ca^{2+} transients could result from nucleotide-dependent regulation of L-type Ca^{2+} channels [B. O'Rourke, P. H. Backx, E. Marban, *Science* **257**, 245 (1992)], sarcoplasmic reticulum Ca^{2+} release channels [G. Meissner and J. S. Henderson, *J. Biol. Chem.* **262**, 3065 (1987)], or metabolite effects on ATP-dependent ion pumps.
11. The oscillations in Ca^{2+} transient amplitude were also eliminated after $I_{K,ATP}$ blockade (Fig. 2B). This may indicate that the primary intracellular oscillator is influenced by surface membrane events, perhaps as a result of secondary ATP consumption by ion pumps such as the Na^+, K^+ ATPase. Tight coupling between Na^+, K^+ ATPase–mediated changes in intracellular ATP and K,ATP channel activity has been demonstrated in the renal proximal tubule [K. Tsuchiya, W. Wang, G. Giebisch, P. A. Welling, *Proc. Natl. Acad. Sci. U.S.A.* **89**, 6418 (1992)]. A second possibility is that glibenclamide may have metabolic effects in addition to its ability to inhibit K,ATP channels [M. Gwilt, B. Norton, C. G. Henderson, *Eur. J. Pharmacol.* **236**, 107 (1993)]. Although there are many alternative explanations as to why inhibiting K^+ efflux halted the oscillations in Ca^{2+} transient amplitude, it is important to note that the reverse was not true, that is, eliminating the Ca^{2+} transients did not eliminate the membrane current oscillations (see Fig. 2C).
12. A. A. Kort, E. G. Lakatta, E. Marban, M. D. Stern, W. G. Wier, *J. Physiol. (London)* **367**, 291 (1985).
13. P. E. Rapp and M. J. Berridge, *J. Theor. Biol.* **66**, 497 (1977).
14. K.-G. Collatz and M. Horning, *Comp. Biochem. Physiol.* **96**, 771 (1990).
15. R. Frenkel, *Arch. Biochem. Biophys.* **125**, 157 (1968).
16. J. Eng, R. M. Lynch, R. S. Balaban, *Biochem. J.* **55**, 621 (1989).
17. V. D. Gooch and L. Packer, *Biochim. Biophys. Acta* **346**, 245 (1974).
18. L. Stryer, *Biochemistry* (Freeman, San Francisco, CA, 1981).
19. The relative ineffectiveness of the ATP in the pipette solution (for example, 5 mM MgATP used in Fig. 1, A and B) to prevent the oscillations and the absence of a rise in the holding current when glycolysis was inhibited with 2-deoxyglucose (Fig. 4D) suggest that the cyclical activation of $I_{K,ATP}$ did not result from subsarcolemmal deprivation of glycolytically derived ATP, but rather from the oscillatory generation of $I_{K,ATP}$ activators such as ADP [J. N. Weiss, N. Venkatesh, S. T. Lamp, *J. Physiol. (London)* **447**, 649 (1992)], AMP, lactate [E. C. Keung, Q. Li, *J. Clin. Invest.* **88**, 1772 (1991)], or protons [W. J. Lederer and C. G. Nichols, *J. Physiol. (London)* **419**, 193 (1989)]. Changes in the concentration of ATP during oscillations in glycolysis (two- to threefold) are much less than those in other intermediates like AMP (20-fold) or fructose 1,6-diphosphate (40-fold) (*4*).
20. A. L. Wit and M. J. Janse, *The Ventricular Arrhythmias of Ischemia and Infarction: Electrophysiological Mechanisms* (Futura, Mount Kisco, NY, 1993).
21. B. Hess, *Hoppe-Seyler's Z. Physiol. Chem.* **364**, 1 (1983).
22. A. Boiteux, A. Goldbeter, B. Hess, *Proc. Natl. Acad. Sci. U.S.A.* **72**, 3829 (1975).
23. M. Markus, D. Kuschmitz, B. Hess, *FEBS Lett.* **172**, 235 (1984).
24. M. A. Aon *et al.*, *J. Cell Sci.* **99**, 325 (1991).
25. K. Tornheim and J. M. Lowenstein, *J. Biol. Chem.* **249**, 3241 (1974).
26. A. Ghosh and B. Chance, *Biochem. Biophys. Res. Commun.* **16**, 174 (1964).
27. B. Chance, B. Schoener, S. Elsaesser, *J. Biol. Chem.* **240**, 3170 (1965); R. Frenkel, *Arch. Biochem. Biophys.* **115**, 112 (1966); B. Chance, B. Schoener, S. Elsaesser, *Biochemistry* **52**, 337 (1964).
28. Results similar to those shown in Fig. 5B were observed in response to photolytic release of ADP in four other cells. When ADP was released during maintained oscillations, phase alterations that included double periodicities were observed. ATP release from caged ATP also induced oscillations in eight cells, but the oscillations began after a longer delay from the time of the flash. Both ADP and ATP influence oscillations in cell-free extracts of glycolytic enzymes (*27*). The delayed effect of ATP may result from its hydrolysis to ADP. Approximately 10% of caged ADP is released by photolysis under optimal conditions and would be likely to be removed within seconds [Y. E. Goldman, M. G. Hibberd, J. A. McCray, D. R. Trentham, *Nature* **300**, 701 (1982)]. The prolonged oscillatory response to the transient perturbation of intracellular nucleotides by flash photolysis is predicted by models of the glycolytic oscillator [A. Goldbeter, in *Mathematical Models in Molecular and Cellular Biology* (Cambridge Univ. Press, Cambridge, 1980), pp. 260–291].
29. We thank A. P. Thomas and W. G. Wier for comments on the manuscript. Supported by NIH grant #RO1 HL 36957.

26 January 1994; accepted 8 July 1994

Transformation of Mammalian Cells by Constitutively Active MAP Kinase Kinase

Sam J. Mansour, Wayne T. Matten, April S. Hermann, Julian M. Candia, Sing Rong, Kenji Fukasawa, George F. Vande Woude, Natalie G. Ahn*

Mitogen-activated protein (MAP) kinase kinase (MAPKK) activates MAP kinase in a signal transduction pathway that mediates cellular responses to growth and differentiation factors. Oncogenes such as *ras, src, raf*, and *mos* have been proposed to transform cells by prolonging the activated state of MAPKK and of components downstream in the signaling pathway. To test this hypothesis, constitutively active MAPKK mutants were designed that had basal activities up to 400 times greater than that of the unphosphorylated wild-type kinase. Expression of these mutants in mammalian cells activated AP-1–regulated transcription. The cells formed transformed foci, grew efficiently in soft agar, and were highly tumorigenic in nude mice. These findings indicate that constitutive activation of MAPKK is sufficient to promote cell transformation.

Cell transformation often results from constitutive activation of components in signaling pathways that control cell proliferation and differentiation. These pathways are initiated from various cell surface receptors, and many converge on the MAP kinase cascade, a module consisting of MAPKK (also known as MAPK or ERK kinase, or as MEK), mitogen-activated protein kinase (MAPK, also known as extracellular signal-regulated kinase or ERK), and pp90 ribosomal protein S6 kinase ($pp90^{rsk}$). These kinases form three successive tiers of a cascade in which MAPKK phosphorylates and activates MAPK, and MAPK phosphorylates and activates $pp90^{rsk}$ (*1*, *2*).

Cellular forms of several viral oncogenes are found as signaling components upstream and downstream of the MAP kinase cascade, which suggests that the pathway mediates cell transformation. Proto-oncogene products upstream of the cascade include

S. J. Mansour, Department of Chemistry and Biochemistry and Department of Molecular, Cellular, and Developmental Biology, University of Colorado, Boulder, CO 80309, USA.
A. S. Hermann, J. M. Candia, N. G. Ahn, Howard Hughes Medical Institute, Department of Chemistry and Biochemistry, University of Colorado, Boulder, CO 80309, USA.
W. T. Matten, S. Rong, K. Fukasawa, G. F. Vande Woude, Advanced BioSciences Laboratories–Basic Research Program, National Cancer Institute–Frederick Cancer Research and Development Center, Frederick, MD 21702, USA.
*To whom correspondence should be addressed.